6th International Conference on Water Resources and Arid Environments (ICWRAE 6): 196-207
16-17 December, 2014, Riyadh, Saudi Arabia

Environmental Impact Assessment of El-Salam Canal on Groundwater Potentiality at Bir El-Abd Rommana Area, Sinai, Egypt

Osama Abdel-Raouf

Water Resource Research Institute (WRRI), NWRC Building, El-Qanater, Egypt

Abstract: The study area is representing the Northern half of Sinai Peninsula. It is considered as a depression and the gradient is from south, to north, the elevation ranges from 20m to zero (sea water level). Generally speaking, utilizing spectral analysis of aeromagnetic data and interpreting conducted geoelectrical resistivity data in addition to hydrochemical analysis of the collected water samples reflect and evaluate the groundwater aquifer properties, water table depths, groundwater salinities and subsurface water fluxes through the area lies between Rommana and Bir El-Abd cities. Also, the study reveals the effect of El-Salam Canal that leads to the mixing of drainage water from areas that cultivated by El-Salam Canal with the brine water which increasing of resistivity toward the south of the study area. The aeromagnetic map of North Sinai was analyzed for identifying the relation between the encountered magnetic anomalies and the causative effects, as well as the separation of the regional and residual magnetic anomalies in relation to the shallow and deep geological features. It indicated that the northern part of the study area is characterized by elongated magnetic anomalies trending in the E-W direction which could be related to the Ragabet El-Naam E-W shear zone, while the southern part of the area shows several circular magnetic anomalies that could be related to strike-slip movements of the Gulf of Aqaba. These results indicated that the depth of the shallow magnetic sources ranges from 1.0 to 3.9 Km, while the depth to the deep magnetic sources ranges from 11.1 to endless Km. The geoelectrical survey is represented also in the form of *thirty two discrete vertical electrical soundings* that was carried out in the considered area around the coastal plain. Nine profiles were constructd, to cover the area around El-Salam Canal. Electrical resistivity soundings data was interpreted qualitatively and quantitatively to detect number of layers or resistivity distribution both laterally and vertically. The geoelectric cross-sections also indicated that the resistivity decreases towards the north due to the salt water intrusion from Mediterranean Sea and decreases to the south. Decreasing of resistivity toward the south may be due to mixing of drainage water from areas cultivated by El-Salam Canal water and/or decreasing of sea water intrusion.

Key words: Groundwater · Aquifer · Environment · Potentiality

INTRODUCTION

The study area, (Figure 1), is located at the Northwestern part of Sinai Peninsula and considered a huge basin of deposition for sedimentary rocks, this column reach about 3000m in depth. The oldest rocks near the southern border of the study area are the Jurassic sedimentary rocks at the core of Gebel El-Maghara. A great thickness of Cretaceous and Tertiary rocks above the Jurassic is observed. The transgression and regression of the Mediterranean Sea play the important role in the hydrogeological conditions that controlling the shallow groundwater aquifer, in that area.

El-Salam Canal goes eastwards to the south of lake Manzala coastal line, going under with the main drains of Lower Serw, Bahr Hadous and Bahr El-Baqar and then goes under Suez Canal through El-Salam Syphon. EL-Sheikh Gaber Canal; the extension to the east of Suez Canal, extends through Northern Sinai plains and ends in Wadi El-Arish, about 145Km to the east of Suez Canal and about 45Km from the Egypt's Eastern international border. El-Salam Canal receives an annual discharge of 1.0 billion m^3 of fresh water from Damietta Branch, along the canal path, another 1.0 billion m^3 of drainage water added from lower Serw and Bahr Hadous main drains at the mixing

Corresponding Author: Osama Abdel-Raouf, Water Resource Research Institute (WRRI), NWRC Building, El-Qanater, Egypt.

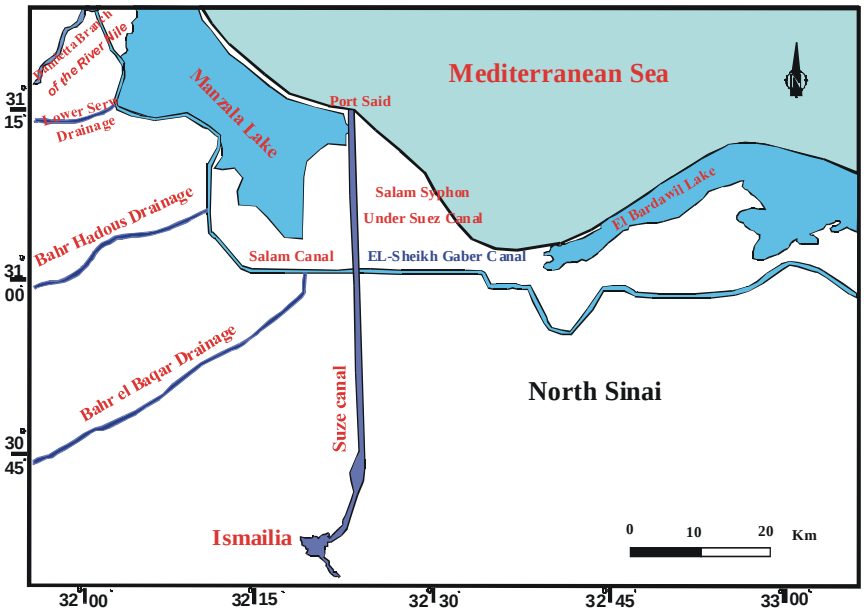

Fig. 1: Location of El-Salam Canal where the study area covers

ratio of 1:1. Reuse of this water can cause negative impacts that, will affect the sustainability of the reclaimed land ecosystems.

El-Salam Canal irrigates most reclaimed lands in the east of the Nile Delta and as it crosses under Suez Canal to its extension in Northern Sinai, which, it is named EL-Sheikh Gaber Canal. The main intake El-Salam Canal of fresh water is located on Damietta Branch of the Nile, 10 Km to the south of its end on the Mediterranean Sea, about 219Km to the west of Suez Canal

Geological Setting: In northern Sinai, Paleozoic deposits not recorded while, the Jurassic was recorded at depth of 3500m and Eocene at depth of 658 m [1].

At the Southern part of Northern Sinai, the Paleozoic rocks are recorded at Nekhel, Abu Hamus and Hamara wells. A major unconformity between the upper clastic Cretaceous and the Triassic deposits is reported from all the drilled wells, this unconformity indicates the late Paleozoic movement, which is called Variscan [2]. The direct evidence for this movement is lacking [3]. The oldest rocks in Northern Sinai are the Triassic, which appear on the surface at Arief El Naga [4].

The geologic map of the study area (Figure 5), indicates that the study area is considered a huge basin of deposition for sedimentary rocks, which is covered by complete geologic column from Recent to Jurassic deposits, the depth of this column reaches to about 3000m. The lithological section represent the study area consists of sand, clay, shale, limestone and chalk. The Quaternary deposits comprise a large thickness; these deposits consist of many cycles of sedimentation of sand clay and silt. Sand dunes covers most of the study area with different thickness increasing toward the north.

Around EL-Bardawil Lagoon, Sabkha deposits were formed due to high rate of evaporation.

Wadi deposits consist of rock fragments, sand, silt and clay and covered by sand dunes, these deposits are very important from hydrogeolgical point of view because its suitability for receiving infiltrated surface water.

Tertiary deposits which consist of clay silt, marl and limestone act as natural barrier of seawater intrusion into sand and clay deposits in north of study.

Miocene and Oligocene deposits consist of clay, shale and chalk, while Eocene and Paleocene deposits consist of limestone and marl.

Upper Cretaceous deposits consists of large section of 700m thickness consists of limestone, clay and chalk. This age include Suder, Matallah, Watta and Halall formations that mainly consist of limestone, marl and dolomite.

The lower Cretaceous deposits(Rizan Unayzah and Malha formation) comprises a great thickness of sand intercalated with shale and limestone.

Magnetic Analysis: The main purpose of this survey was to delineate the regional subsurface structure of the area. (Fig. 3) shows the aeromagnetic map of the Sinai area.

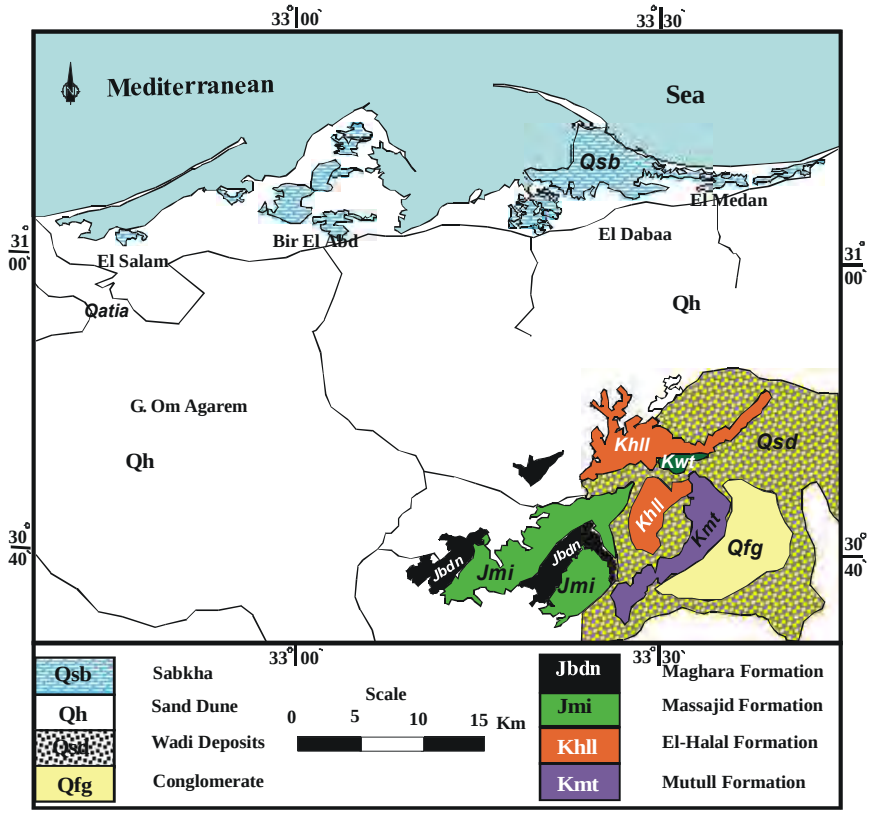

Fig. 2: Geologic Map of the study area *after Egyption Geological Survey 1992

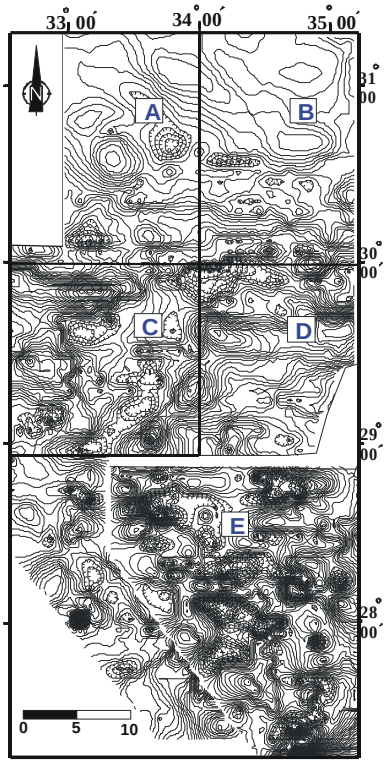

Fig. 3: Aeromagnetic map of Sinai area (after geologic survey of Israel 1980)

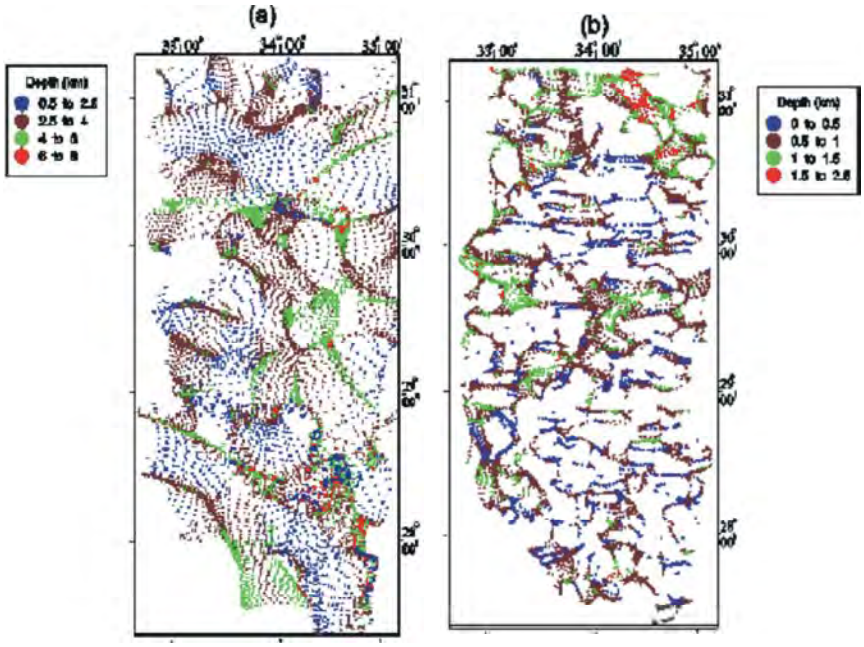

Fig. 4: Solutions of Euler obtained from
a) Regional magnetism, b) residual magnetism

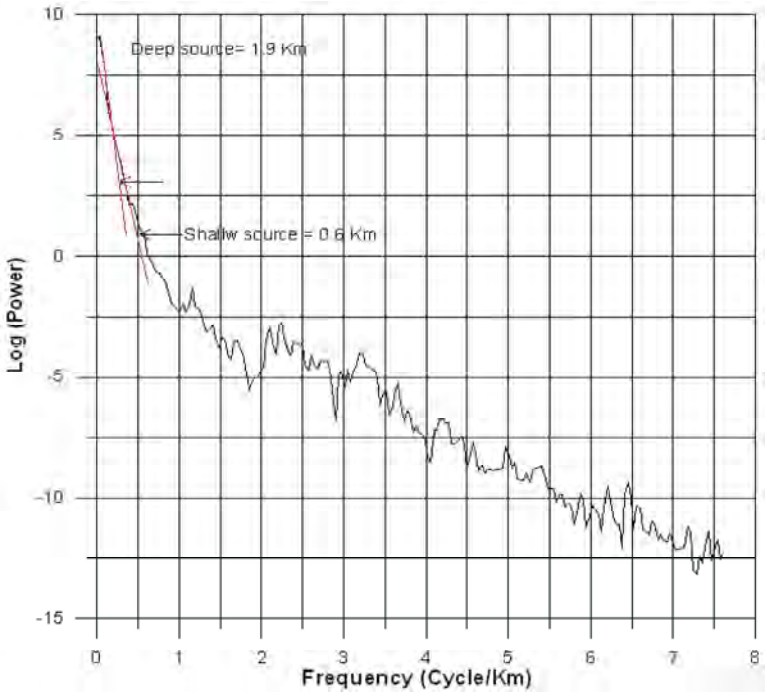

Fig. 5: Average power spectrum of aeromagnetic anomaly map for the grid A

The northern part of the map area is characterized by elongated magnetic anomalies trending in the E-W direction. It should be stated that the magnetic trends do not occur randomly but are aligned along definite and preferred axes forming trends that can be used to define magnetic provinces [6, 7]. The E-W trend could be related to the Ragabet El-Naam E-W shear zone [8]. Other circular anomalies were observed and could be interpreted as uplifting basement or intrusion of dibasic dykes.

Table 1: Results of spectral analysis and depth estimations for the grids A, B, C, D and E

		Shallow sources depths		Deep sources depths	
Grid	Peak value (Cycle/km)	To top	To bottom	To top	To bottom
A	0.02209697	1.9	18.2	5.1	9.9
B	0.0204692	2.03	19.7	5.2	11.1
C	0.0267438	3.9	11.4	6.1	6.9
D	0.0256348	2.07	13.9	4.6	8.1
E	0.0416667	3.1	6.2	4.7	Endless

* All depths are in km.

Analyses of this map include structural interpretation using Euler deconvolution method [9]to delineate the magnetic contacts (faults) and as well as their depths and power spectral method was used to estimate the depth to Curie point from magnetic data.

(Fig. 4) show the Euler solutions for the regional and residual data, respectively. Good clustering of the solutions was obtained from regional magnetic data. These solutions show several trends (E-W, NW-SE, NE-SW and N-S) and having a depths ranged between 2.5-8.0km.

Spectral analysis was used to estimate the Curie-point isotherm depth, [10], [11] and [12]. Estimates of the thickness of the magnetized portion of the earth's crust suggest that there are two types of lower boundaries of the layer of the magnetized rocks.

The study area was divided into 5 grids Labeled A, B, C, D and E on (Fig. 3). For each grid, power spectrum was calculated and depth to the Curie point was estimated for both shallow and deep sources. These results are listed in (Table 1) (Fig. 5) shows an example of radically power spectrum for grid.

Geoelectric Resistivity Survey: The basic principles of the geoelectrical resistivity techniques have been discussed by many authors among them. Flathe [13], Parasnis [14], Zohdy *et al*. [15], Telford, *et al*. [16] and Apparao [17]. Geoelectrical resistivity surveys in the form of thirty two discrete vertical electrical soundings were carried out in the considered area around the coastal plain of the Mediterranean Sea (Fig. 6). The well-known Schlumberger configuration with current electrode spacing (AB) starting from 3 m up to 600m, in successive steps, is selected and applied. Nine profiles were constructed, to cover the area around El-Salam Canal (Fig. 6).

The interpretation of the acquired resistivity sounding data was carried out both qualitatively and quantitatively to represents the horizontal and vertical variations of resistivity. Iterative and indirect procedure is used to invert the acquired resistivity data. The basic theory of this technique assumes that, the subsurface model consists of a finite number of layers separated by horizontal interfaces. Qualitatively, Eight resistivity pseudo-sections are constructed to delineate variations in apparent resistivity across the study area. They are characterized by homogenous apparent resistivity distribution with an average value of 25Ω.m. in most sections and very high apparent resistivity of ranging between 140 and 500Ω.m for the surface layer in the others. Figures (7), (8) and (9) represent three of these pseudo sections.

Vertical Distribution of Resistivity: Quantitatively, to demonstrate the distribution of the calculated resistivity parameters (true resistivity and thickness) in the vertical plane across the study area, eight geoelectric resistivity cross-sections are constructed covering the study area. In fact, the trends of the previously discussed resistivity pseudo-sections are followed in constructing the cross-sections (Fig. 10-12). In the cross sections, the plotted vertical scale represents the elevation in meters relative to the sea level and the plotted horizontal scale represents the horizontal distance in meters between the conducted soundings along the section. The geoelectric cross sections indicated four-geoelectric units are picked.

The first surface layer have a true resistively values ranges from 145.4 to 417.1Ω.m. and thickness of about 2m. This unit can be interpreted as the uppermost friable, dry part of sand dunes. The resistivity values of this unit may be due to the effect of irrigation water in some parts.

The second unit has a true resistivity ranging from 80.7Ω.m. to 851.8?.m. and can be interpreted as dry sandy layer. This unit may contain fresh groundwater at the section of VES's 26 and 27.

The third geoelectric unit, which comprises true resistivity values ranging from 150 to 176Ω.m. and thickness ranges from 15 to 40m, is equivalent to the water-bearing zone of sand dunes. It is clearly noticed that the resistivity of this unit decreases towards the northeast, because it is closer to the Mediterranean Sea.

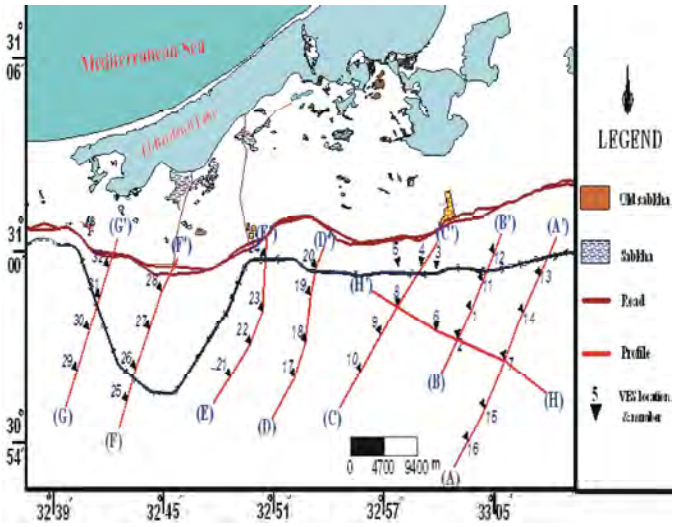

Fig. 6: Locations of resistivity profiles'

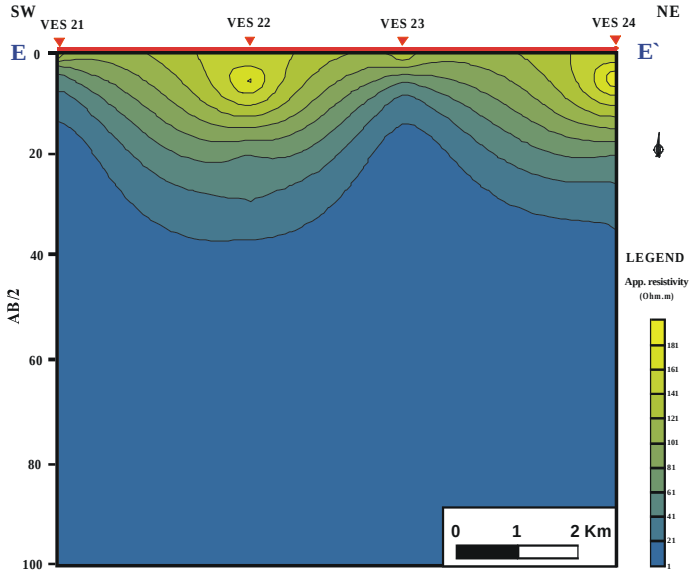

Fig. 7: Geoelectric resistivity pseudo-section EE'

The fourth unit has very low true resistivity values (> 10Ω.m.) and is considered the base of the investigated depth interval. Based on the available information of drilled wells in the study area, this unit can be represented by clayey deposits.

Iso-Pach Map of the Aquifer: This map, (Fig. 13) was constructed to indicate the thickness of the third layer which was considered as the main water bearing layer in the investigated section. It represents that this thickness decrease toward the northeast and west, while increases to the middle and southeast. The maximum thickness of this layer reached about 35m south of El-Negela, El-Kherba cities and Bir El-Abd cities. Also, it is clearly noticed that there are some areas of more than 40m in the form of basins appear as closed contours of high values south of Rabaa city. Northward of these basins, lower contour values closed loops are located. Generally the thickness of this layer is controlled by the relief of the underlined clayey layer. The thickness of the third layer can be presented as 3-dimensional block diagram (Fig. 14).

Iso-Salinity Contour Map: Based on the resistivity sounding data, the Iso-salinity contour map (Fig. 15) was constructed. It shows that the low salinity water (< 2,000mg/l) is found in the western part of the studied area, while the eastern part comprises higher salinity due to the effect of brdaweel Lake.

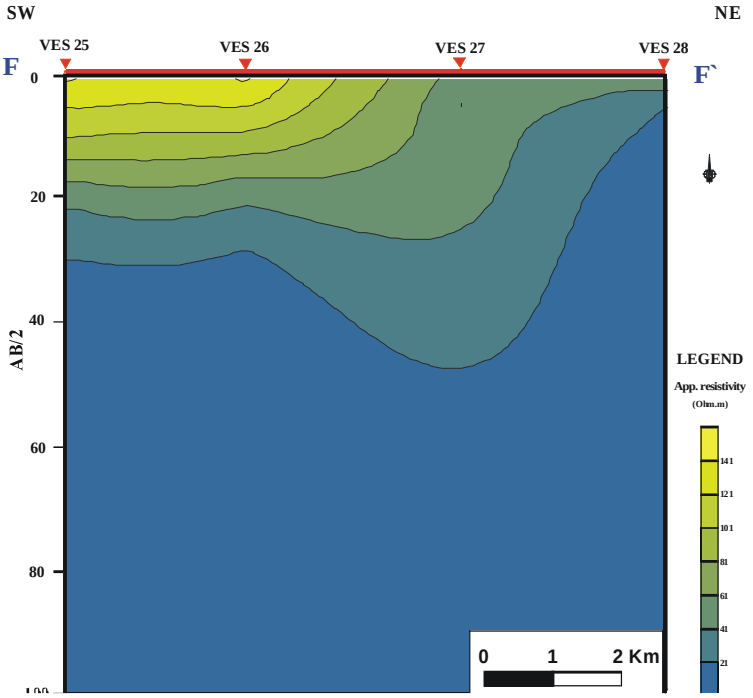

Fig. 8: Geoelectric resistivity pseudo-section FF'

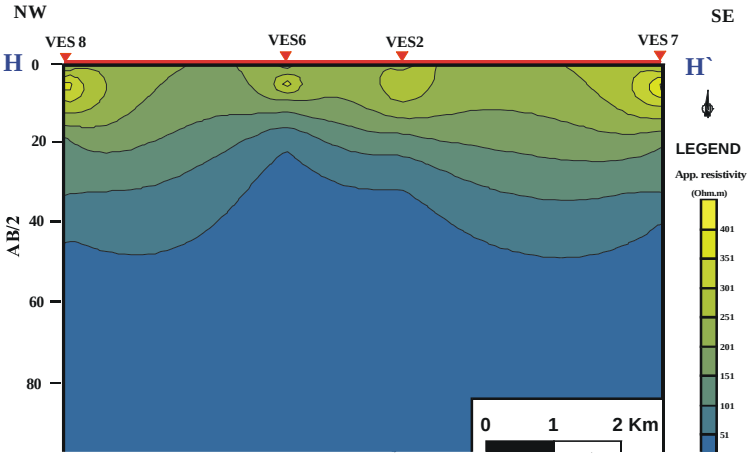

Fig. 9: Geoelectric resistivity pseudo-section HH'

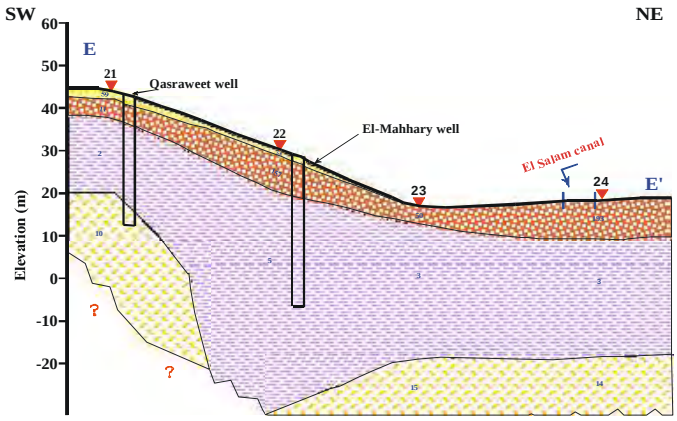

Fig. 10: Geoelectric cross section E E

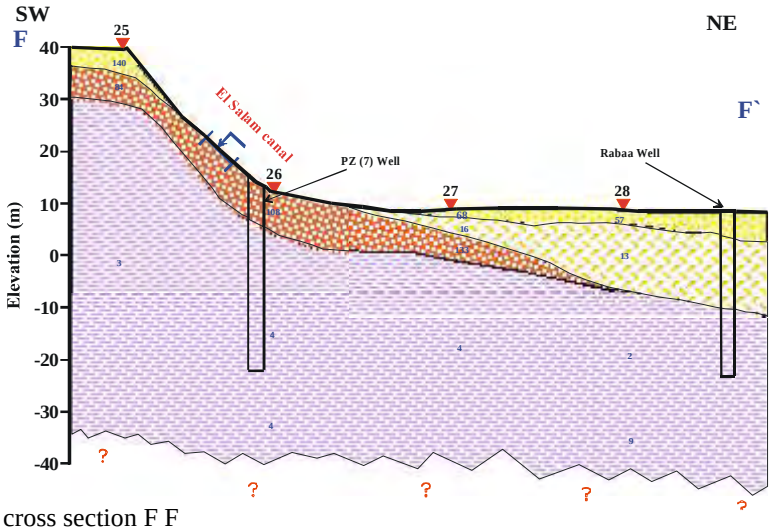

Fig. 11: Geoelectric cross section F F

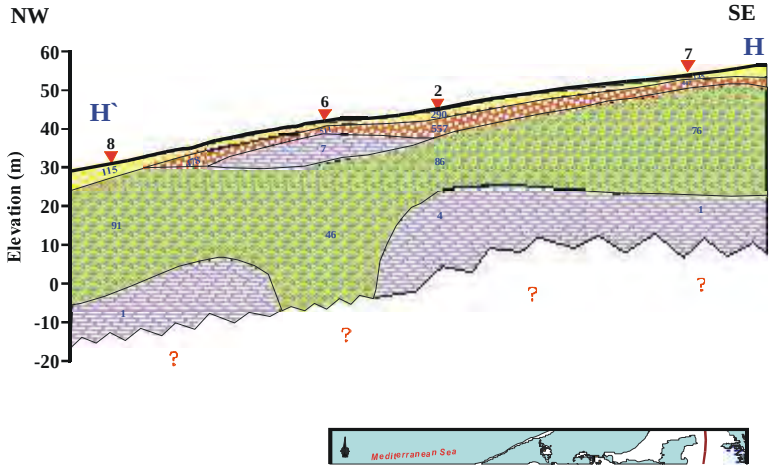

Fig. 12: Geoelectric cross section H H

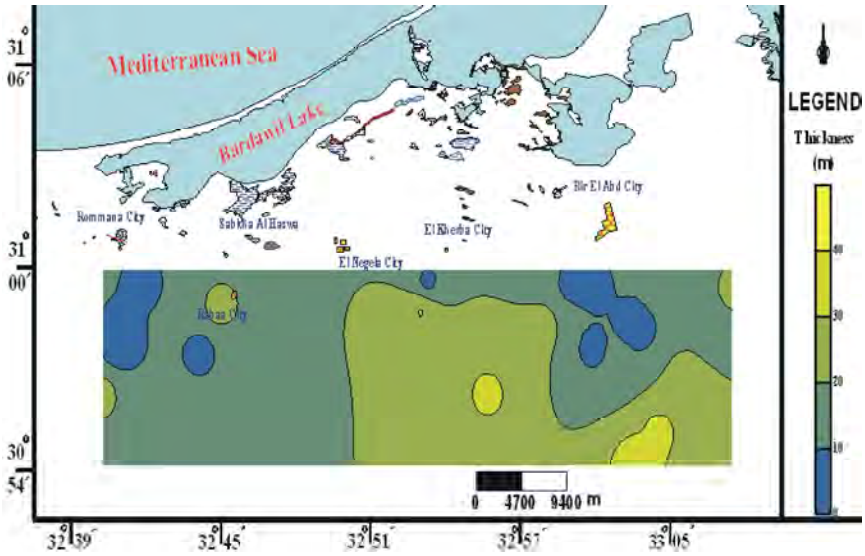

Fig. 13: Thickness contour map of the aquifer

Table 2: Aquifer hydraulic parameters of some wells in the study area

Well name	Storage coefficient	Transmissivitym²/d	Well loss D²/m⁵	Fm. loss D/m²
El Naser	0.041	1510	7.1 * 10^{-7}	0.00325
Qatia	0.039	1767	3.5* 10^{-7}	0.00436
El Meriah	0.037	710	2.85* 10^{-7}	0.00199
El Masharif	0.00716	578	4.14* 10^{-7}	0.00519

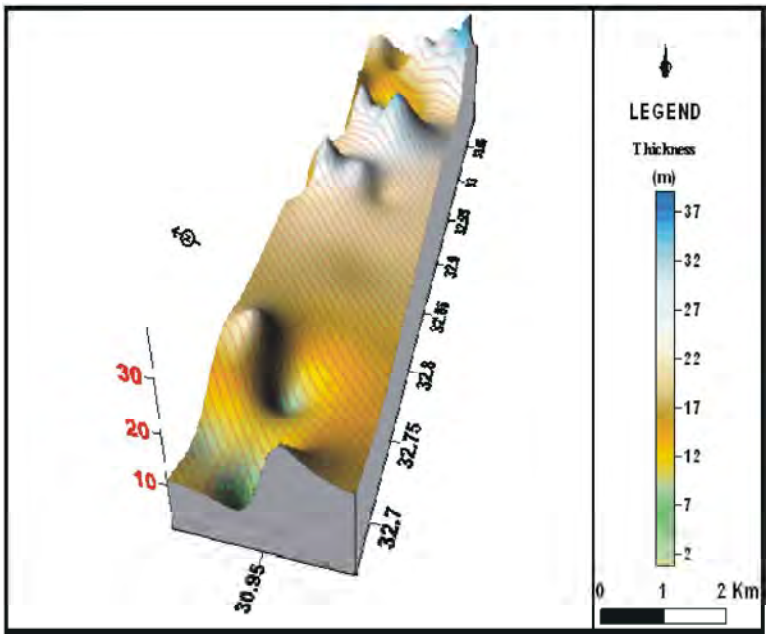

Fig. 14: 3D block diagram of aquifer thickness

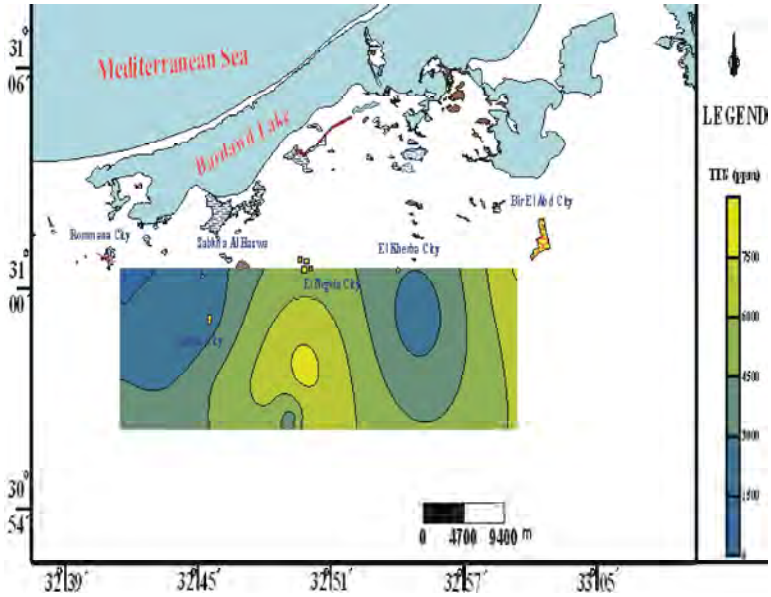

Fig. 15: Iso-Salinity of the study area

Hydrogeological Settings: The old stabilized sand dune aquifer is the main aquifer at the area. This aquifer consists of sand and silt. The aquifer exists at some areas in the form of lenses, connected or disconnected. The main source of recharge to this aquifer is the rainfall and return irrigation water. This aquifer was classified into three zones as follows.

First zone; of friable sand, silt and clay at its lower part. The thickness of this zone ranges between 20m due north and at coastal zone to 100m due South at Maghara mountain, with distance 60Km between them, the infiltrated water passing from this zone to the second zone directly.

Second zone; is considered the lower part of first zone, the thickness of this zone reaches 20m and considered the main aquifer in the study area. The aquifer is unconfined. The salinity of the water into this zone ranges between 2000 and 4000ppm.

The third zone; represents isolated sand lenses between clay layers, ranges between 20-140m. with few meters thickness. The salinity of water reaches 10.000ppm, due to the effect of sea intrusion.

Aquifer Hydraulic Parameters: From the available water wells in the study area, Table (2) shows the measured aquifer hydraulic parameters of these wells. There is great difference between hydraulic parameters of the same aquifer especially the transmissivity values from the test wells which drilled by *WRRI*, the values of transmissivity ranges between 578m^2/d at Masharif well to 1767m^2/d at Qatia well. The storage coefficient ranges between $716x10^{-2}$ to $37x10^{-1}$ at EL-Masharif wells and Meriah wells respectively. Meanwhile, the well number increase randomly in the last 15 years due to the low cost of well construction.

Through the flow up of the aquifer during last 25 years, it was found that the water table is affected directly by rainfall and from winter to summer season. The water level ranges between 2 and 6m above mean sea level, but in some parts this level underlay the sea level (at EL-Shohat area).

The flow direction is generally towards North but in sabkha areas, this flow towards these sabkhas (low lands or Hods).

Water Quality: The quality of water is the main important factor in the evaluation of this aquifer especially; this aquifer extends along the Mediterranean Sea. There are three water types included into this aquifer, first, water of 2500-3000ppm. (Total dissolved solids) at the shallow layer and appears at the surface in some areas. Second, the water of 300-5000ppm, this type of water occurs at depth of 20m. (main aquifer), the third type is of salinity reaches 30.000ppm and occurs at depth ranges from 30-140m. The predominant cations are Mg-Na due to the presence of saline water from the local lakes and the Mediterranean Sea. The predominant cations are Mg-Na due to mixing between seawater and rainwater and dissolution of magnesium rocks that included the aquifer sediments.

By applying Sulin's graph on the present groundwater samples, the water origin could be determined for the different localities. The hydrochemical composition of the groundwater of the study area (North Sinai) reflects the Na_2SO_4- water type that indicates deep meteoric genesis. It is represented by Rommana and El Mahhary water wells, while, composition referring to recent marine water genesis where rCl - r(Na + K) /Mg <1, is dominant in groundwater of El-Shohat, Qatia, Bir El-Abd and kasraweet wells.

Environmental Impacts: Due to the presence of El-Salam canal, the hydrogeological condition of the dune aquifer will be affected by the irrigation water from this canal. The irrigation water will be infiltrated into the aquifer and will cause environmental impact to the aquifer.

The Sand dunes receive all the rainwater and infiltrating to the lower layers. The calculated volume is estimated by 15 million m^3/year from the hydrologic study.

Return irrigation water and septic tanks (50%) feed the aquifer due to the high infiltration rate. After the compilation of EL-Salam canal, this very important the expected volume is estimated by (5 million m^3/year). The total recharge volume to the aquifer is equal to 20 million m^3/year, hence there is a great difference between the recharge and discharge (9-10) million m3/year The great extension of the area (3000/km^2) plays an important role in the distribution of the fresh water layer as a thin film on the saline water layer; hence, the pumping rate must be controlled to avoid the sea water intrusion and deterioration of the aquifer.

The constructed iso-salinity map that based on the resistivity data closely confirmed the salinity map which constructed from the analyzed water samples.

Chemical analyses of the collected water samples was done to assess the groundwater quality and to determine the suitability of water for drinking and irrigation. The study revealed the following:

- The pH value ranges between 7.01 to 8.20 with an average of 7.605. This is due to the difference in chemical composition of aquifer rocks. All the groundwater samples in the study area are suitable in all purposes.
- The conductivity of groundwater in the study area ranges from 2.07 to 13.05 mS/cm with an average of 7.6mS/cm.

- The salinity of groundwater in the study area ranges from 1435 to 8358mg/L with an average of 4896.5mg/L.
- The content of Potassium ranges between 7.8 to 39mg/L with an average of 23.4mg/L.
- Sodium content in the groundwater of the study area is high and varies from 161 to 2489mg/L with an average of 1325mg/L.
- The Magnesium content in the groundwater of the study area changes from 36 mg/L to 396mg/L with an average of 216mg/L. The increment of magnesium content is due to the seepage of saline water from the Bardaweel Lake to the aquifer.
- Calcium ion ranges from 120 to 780mg/L with an average of 450mg/L.
- The Chloride content in the study area varies between 213 and 5077mg/L with an average of 2645mg/L. The increment of chloride content is due to the seepage of saline water from the Bardaweel lake Mediterranean Sea to the aquifer.
- The Sulfate content in the study area ranges from 144mg/L to 1584mg/L with an average of 864mg/L.
- The Bicarbonate content varies between 122 and 366mg/L with an average of 244mg/L.
- In the present study, the groundwater salt types were determined as sodium chloride and calcium sulphate. By applying the Sulin's graph, the origin of water is meteoric water and due to the sea water intrusion in some localities.

It can be concluded that the study reveals the effect of El-Salam Canal that leads to the mixing of drainage water from areas that cultivated by El-Salam Canal with the brine water which increasing of resistivity toward the south of the study area.

REFERENCES

1. Said, R., 1962. The Geology of Egypt, Elsevier publishing Company, Amsterdam, New York.
2. **Missing**
3. SAbu El Ata Ahmad S., 1973. A coordination between field data and subsurface geology of Gilbana – Bir El Abd – Gifgafa area Northwest Sinai, A.R.E., M. Sc. Ain Shams Univ., Fact. Of Scie., Egypt.
4. Awad, G.H., 1946. On the occurrence of marine Triassic (Mushelkalk) deposits in Sinai. Bull. Inst. Egypt, 27: 397-429.
5. Geological survey of Egypt, 1993. Geological map of Sinai Peninsula, sheet no.5, scale 1:500,000.
6. Affleck, J., 1963. Magnetic anomaly trend and spacing pattern: Geophysics, 28: 379-395.
7. Hall, S.A., 1979. A total intensity aeromagnetic map of the Red Sea and its interpretation: USGS, Saudi Arabian project Report, pp: 265-275.
8. Steintiz, G., Y. Bartove and J.C. Hunziker, 1978. K/Ar age determination of some Miocene-Pliocene basalts in Israel: their significance to the tectonic of rift valley. Geologic Magazine, 115: 329-340.
9. Reid, A.B., J.M. Allsop, H. Granser, A.J. Millett and I.W. Somerton, 1990. Magnetic interpretation in three dimensions using Euler deconvolution. Geophysics, 55: 80-9.
10. Boler, F.M., 1978. Aeromagnetic measurements, magnetic source depths and Curie point isotherm in the Vale-Omyhee, Oregon. M.S. thesis, Oregon State Univ., Corvallis.
11. Smith, R.B., R.T. Shuey, R.O. Fridline, R.M. Otis and L.B. Alley, 1974. Yellowstone hot spot. New magnetic and seismic evidence. Geology, 2: 451-455.
12. Salem, A., K. Ushijima, A. Elsirafi and H. Mizunaga, 2000: Spectral analysis of aeromagnetic data for geothermal reconnaissance of Quseir area, northern Red Sea, Egypt. Proceeding World Geothermal Congress, 1969-1674.
13. Flathe, H., 1976. The role of a geologic concept in geophysical research work solving hydrogeological problems. Geoexplor., 14: 195-206.
14. Parasnis, D.S., 1979. Principles of applied geophysics. Champan and Hall, Halsted Press Book, John Wiley and Sons, New York.
15. Zohdy, A.R., G.P. Eaton and D.R. Mabey, 1974. Application of surface geophysics to groundwater investigations. USGS techniques of water- resources investigations. Book 2 Chap., pp: 116.
16. Telford, W.L. Geldart and R. Sheriff, 1990. Applied geophysics. Second Ed., Cambridge Univ. Press, pp: 660.
17. Apparao, A., 1991. Geoelectric profiling. Geoexploration, 27: 351-389.
00. Ghosh, D.P., 1971. “The application of linear filter theory to the direct interpretation of geoelectrical resistivty sounding measurements”: Geophysical Prospecting, XIX(2): 192-217.
00. Research Institute For Water Resources, 1988. Groundwater management study in El Arish – Rafah Plain area, phase 1, interim, report Marsh 1988. Internal report, El-Kanater El- Khyria, WRC. Egypt.
00. Aeromagnetic map of Sinai; 1:500 000. 1980. Geologic Survey of Israel.

00. Said, R., 1990. Geological evaluation of the River Nile. Springer-Verlag, Pub., New York, Heidlberg, Berlin, pp: 121.
00. Sulin, V.A., 1948. Condition of formation principals of classification and constituents of natural waters, particularly water of petroleum accumulation Moscow. Leningrad, Acad. of Sc., USSER.
00. Mohamed, A.K., 2003. Evaluation of borehole geophysical well logging and discrete surface resistivity sounding for stratigraphic mapping in Wadi Feiran, Sinai, Egypt, 3rd international symp. On Geophys., Tanta University, Egypt.
00. Flathe, H., 1955a. "Possibilities and limitations in applying geoelectrical methods to hydrogeological problems in the coastal areas of northwest Germany": Geophys. Prosp. III, pp: 95-105.
00. Flathe, H., 1955b. "A practical method of calculating geoelectrical model graphs for horizontally stratified media": Geophys. Prosp. III, pp: 268-294.